

DOCUMENT 810-5, REV. D; VOL. I  
DSN/FLIGHT PROJECT  
INTERFACE DESIGN

TCI-40, REV. C  
DSN TELECOMMUNICATIONS INTERFACES  
ATMOSPHERIC AND ENVIRONMENTAL EFFECTS

(Insert this modular document in your 810-5; Rev. D; Vol. I Handbook)

RELEASE DATE: May 1, 1992

---

Prepared by: S.D. Slobin  
S. D. Slobin

Approved by: P. L. Parsons  
P. L. Parsons

A. PURPOSE

This module presents atmospheric, environmental, and extraterrestrial effects of concern to the Deep Space Network (DSN) telecommunications link.

B. SCOPE

Statistics of atmospheric attenuation and noise temperature at each tracking antenna site are presented for those microwave frequencies used by the DSN. In this module, the values of attenuation and noise temperature increase are given relative to a no-atmosphere (vacuum) condition. This presentation is thus compatible for use with the vacuum gain and noise temperature presentations of antenna performance given in Modules TCI-10 (70-meter antennas) and TCI-30 (34-meter antennas). The DSN 26-meter antennas are described in Module TCI-20 of this volume. Gain and noise temperature values are presented for average clear-sky conditions only (cumulative distribution = 0.25).

Statistics of wind speed are given. These are used both to determine the statistics of antenna gain loss due to wind loading and also to ascertain the percentage of time an antenna will be unusable due to excessive wind speed.

Extraterrestrial effects are primarily the increased system noise temperature due to hot body noise from the sun, moon, planets, and radio sources. These effects are significant only when the antenna beam is in the vicinity of these noise sources during tracking of spacecraft.

Charged-particle effects are given in Module TCI-50, Solar Corona Solar Wind Effects.

C. LOCATION OF MATERIAL

1. Contents

<u>Designator</u>	<u>Title</u>	<u>Page</u>
-------------------	--------------	-------------

D. GENERAL INFORMATION

1.	Atmospheric Attenuation and Noise Temperature .....	3
a.	General Description .....	3
b.	Calculation of Mean Atmosphere Physical Temperature .	6
c.	Elevation Angle Modeling .....	6
d.	Calculation of Noise Temperature From Attenuation ..	7
e.	Cosmic Background Adjustment .....	7
f.	Signal-to-Noise Ratio Degradation .....	7
g.	Example of Use of Attenuation Statistics .....	8
2.	Wind Loading .....	9
3.	Hot Body Noise .....	9
a.	Solar Noise .....	9
b.	Lunar Noise .....	11
c.	Planetary Noise .....	11

2. Illustrations

<u>Figure</u>	<u>Title</u>	<u>Page</u>
1.	Cumulative Distribution of Total Zenith Attenuation for S-band and X-band.....	14
2.	Cumulative Distribution of Total Zenith Attenuation for Ka-band .....	15
3.	Probability Distribution for Wind Conditions at Goldstone	16
4.	Typical 26-meter S-band Antenna Pattern Showing Sidelobe Structure.....	17
5.	Solar Radio Flux (SFU) at 2800 MHz, (10.7 cm Wavelength) During Solar Cycles 18 Through 22 (Present) .....	18
6.	DSS-15 X-band System Noise Temperature Increases Due to the Sun at Various Offset Angles, Showing Larger Increases Perpendicular to Quadripod Directions .....	19
7.	DSS-16 S-band Total System Noise Temperature at Various Offset Angles From the Sun .....	20
8.	DSS-12 S-band Total System Noise Temperature at Various Declination and Cross-Declination Offsets From the Sun ..	21

9.	DSS-12 X-band Total System Noise Temperature at Various Declination and Cross-Declination Offsets From the Sun ..	22
10.	Total S-band System Noise Temperature for 70-meter Antennas Tracking Spacecraft Near the Sun (Derived from 64-meter measurements) .....	23
11.	X-band Noise Temperature Increase for 70-meter Antennas as a Function of SEP Angle, Nominal Sun, 23,000 K Disk Temperature .....	24
3.	Tabular Data	

<u>Table</u>	<u>Title</u>	<u>Page</u>
1.	S-band (2295 MHz) Atmosphere Noise Temperature and Attenuation at Zenith .....	5
2.	X-band (8420 MHz) Atmosphere Noise Temperature and Attenuation at Zenith .....	5
3.	Ka-band (32 GHz) Atmosphere Noise Temperature and Attenuation at Zenith (see Figure 2) .....	6
4.	Parameters for X-band Planetary Noise Calculation plus Sample X-band Noise Temperature Contributions .....	13

#### D. GENERAL INFORMATION

##### 1. Atmospheric Attenuation and Noise Temperature

a. General Description. The atmosphere models presented herein give S-band (2295 MHz), X-band (8420 MHz), and Ka- band (32 GHz) atmosphere noise temperature and attenuation. The noise temperature effects are added to the "vacuum" noise temperature condition of the antenna, as given in Modules TCI-10 (70-meter) and TCI-30 (34-meter). The attenuation values are subtracted from the "vacuum" condition gain values, as given in TCI-10 and TCI-30. It should be noted that simple atmosphere models (vacuum, 0% least effect weather, 25% average clear, 50%, 80%, and 90% cloudy, no rain) are also given in the 70-meter antenna module TCI-10, Rev. E, and in the 34-meter antenna module TCI-30, Rev. D. Those models are adequate for quick estimation of link performance, but the use of a single atmosphere noise temperature parameter  $T_z$  in elevation angle modeling is strictly not correct. As the Sand X-band weather effects up to 90% weather are small anyway, this leads to small errors in calculation of system noise temperature at low elevation angles. For Ka-band, the errors will be substantially larger. Elevation angle modeling should be done using attenuation only; this will be discussed below.

The Ka-band model is based on actual water vapor radiometer noise temperature measurements made near 32 GHz at the Madrid and Canberra DSN sites. As both sets of measurements yielded similar statistical results, a single atmosphere model was created for those sites. A statistical attenuation model was deduced from the noise temperature measurements. Goldstone has only

one-sixth as much rain as do the other sites (3.5 inches per year versus about 21 inches) and thus has far more benign weather. A conservative

Ka-band model for Goldstone with lesser noise temperature and attenuation was deduced from the Canberra/Madrid measurements by taking one-third of the Canberra/Madrid increases above baseline as being representative of the Goldstone weather model. This method yields statistical results which match results of limited water vapor radiometer measurements at Goldstone in 1981.

The X-band model was deduced from the Ka-band model as follows: the Ka-band baseline oxygen-only attenuation was subtracted from the measured Ka-band statistical attenuation values. The remainder (water vapor and liquid water effect) was reduced by frequency-squared (14.44) to give the X-band vapor plus liquid contribution. The baseline X-band oxygen-only attenuations for Goldstone and Canberra/Madrid were added to give the total attenuation statistics for X-band. The X-band noise temperatures were calculated from the attenuation values. The two S-band models were created in a manner similar to that described above. The atmosphere models for a particular complex (e.g., Goldstone) should be used for all antennas at that complex (e.g., DSS 14, DSS 15, etc.).

Table 1 gives the S-band (2295 MHz) atmosphere noise temperature and attenuation at zenith as a function of weather condition (cumulative distribution, CD). As an example, CD - 0.90 (90-percent weather) means that 90-percent of the time a particular weather effect (noise temperature or attenuation) is less than or equal to a given value. Conversely, that particular effect is exceeded only 10 percent of the time. There are two models: Goldstone and Canberra/Madrid.

Qualitatively, the weather condition (cumulative distribution) is described as follows:

CD - 0.00	clear dry, lowest weather effect
CD - 0.25	average clear weather
CD - 0.50	clear humid, or very light clouds
CD - 0.90	very cloudy, no rain
CD > 0.95	very cloudy, rain

By their very natures, clouds and rain are poorly modeled; and the water vapor radiometer data used here are sparse for the larger weather effects exceeded only 5 percent of the time.

Table 2 gives the X-band (8420 MHz) atmosphere noise temperature and attenuation at zenith as a function of weather condition. There are two models: Goldstone and Canberra/Madrid. Table 3 gives the Ka-band (32 GHz) total atmosphere noise temperature and attenuation at zenith as a function of weather condition. There are two models: Goldstone and Canberra/Madrid.

Figure 1 shows the cumulative distribution of total zenith attenuation for S-band at Goldstone, S-band at Canberra/Madrid, X-band at Goldstone, and X-band at Canberra/Madrid. Figure 2 shows the cumulative distributions for Ka-band at Goldstone and at Canberra/Madrid. Noise temperature curves are not

Table 1. S-band (2295 MHz) Atmosphere Noise Temperature and Attenuation at Zenith (see Figure 1)

CD	Noise Temperature (K)		Attenuation (dB)	
	Goldstone	Canberra/Madrid	Goldstone	Canberra/Madrid
0.00	1.770	1.867	0.02910	0.03070
0.10	1.785	1.893	0.02919	0.03096
0.20	1.799	1.915	0.02925	0.03114
0.25	1.805	1.924	0.02927	0.03120
0.30	1.811	1.932	0.02928	0.03125
0.40	1.823	1.950	0.02932	0.03136
0.50	1.836	1.967	0.02936	0.03147
0.60	1.848	1.985	0.02939	0.03157
0.70	1.861	2.005	0.02944	0.03173
0.80	1.877	2.032	0.02953	0.03198
0.90	1.899	2.079	0.02972	0.03255
0.95	1.926	2.151	0.03006	0.03358
0.98	1.968	2.270	0.03067	0.03540
0.99	1.999	2.362	0.03114	0.03682
0.995	2.061	2.547	0.03210	0.03969
0.998	2.281	3.203	0.03552	0.04997

Table 2. X-band (8420 MHz) Atmosphere Noise Temperature and Attenuation at Zenith (see Figure 1)

CD	Noise Temperature (K)		Attenuation (dB)	
	Goldstone	Canberra/Madrid	Goldstone	Canberra/Madrid
0.00	2.006	2.097	0.0330	0.0345
0.10	2.089	2.325	0.0342	0.0380
0.20	2.149	2.482	0.0350	0.0404
0.25	2.170	2.534	0.0352	0.0411
0.30	2.191	2.585	0.0355	0.0419
0.40	2.233	2.689	0.0359	0.0433
0.50	2.276	2.794	0.0364	0.0448
0.60	2.318	2.900	0.0369	0.0462
0.70	2.374	3.045	0.0376	0.0483
0.80	2.458	3.273	0.0387	0.0516
0.90	2.633	3.775	0.0413	0.0593
0.95	2.933	4.660	0.0459	0.0731
0.98	3.455	6.205	0.0540	0.0974
0.99	3.861	7.408	0.0603	0.1165
0.995	4.676	9.813	0.0732	0.1550
0.998	7.573	18.250	0.1191	0.2928

Table 3. Ka-band (32 GHz) Atmosphere Noise Temperature and Attenuation at Zenith (see Figure 2)

CD	Noise Temperature (K)		Attenuation (dB)	
	Goldstone	Canberra/Madrid	Goldstone	Canberra/Madrid
0.00	5.016	6.070	0.0830	0.1006
0.10	6.071	9.157	0.1001	0.1519
0.20	6.790	11.236	0.1115	0.1860
0.25	7.020	11.888	0.1150	0.1965
0.30	7.251	12.542	0.1184	0.2070
0.40	7.715	13.854	0.1254	0.2279
0.50	8.182	15.172	0.1324	0.2488
0.60	8.652	16.497	0.1393	0.2697
0.70	9.311	18.362	0.1493	0.2996
0.80	10.351	21.321	0.1654	0.3478
0.90	12.673	27.897	0.2023	0.4584
0.95	16.759	39.260	0.2688	0.6580
0.98	23.786	58.017	0.3860	1.0100
0.99	29.156	71.680	0.4778	1.2851
0.995	39.632	96.704	0.6630	1.8407
0.998	73.681	164.081	1.3264	3.8307

shown. A rule of thumb linking attenuation and noise temperature is that 1 dB of atmospheric attenuation causes about 60 Kelvins of noise temperature. This relationship is nearly linear over the range 0 to 1 dB.

For other nearby frequencies within the S-, X-, and Ka-bands, the weather-effects models presented here should be used without modification.

b. Calculation of Mean Atmosphere Physical Temperature. The mean physical temperature of the atmosphere is modeled to be a function of weather condition, or cumulative distribution. This reflects the assumption that those effects which are of larger value (e.g., high noise temperature) occur closer to the surface and hence are at a higher average temperature than those which have a lesser effect. The mean atmosphere physical temperature is given by:

$$T_p = 265 + 15 * CD \text{ (Kelvins)}$$

where CD - cumulative distribution of weather effect (0-1)

Note that the maximum value of  $T_p$  is 280 K.

c. Elevation Angle Modeling. Only the attenuation should be modeled as a function of elevation angle. The atmosphere noise temperature contribution at any elevation angle can be calculated from the modeled attenuation at that elevation angle. A flat-earth model is used here, wherein the attenuation increases with decreasing elevation angle:

$$A(\emptyset) = A_{zen}/\sin(\emptyset) \text{ (dB)}$$

where  $A_{zen}$  = zenith atmosphere attenuation (dB), as given in Tables 1, 2, and 3

and  $\emptyset$  = elevation angle of antenna beam

The flat-earth approximation is valid to within 1%-3% at 6 degrees elevation angle.

d. Calculation of Noise Temperature From Attenuation. An attenuating medium creates a noise temperature effect which adds to system temperature. The atmosphere noise temperature at any elevation angle is calculated from the attenuation by:

$$T_{atm} = T_p * (1 - 1/L) \text{ (Kelvins)}$$

where  $T_{atm}$  =  $T_p * (1 - 1/L)$  (Kelvins)

$T_p$  = mean physical temperature of atmosphere, calculated above

$L$  = loss factor of atmosphere ( $>1.0$ ) -  $10^{A(\emptyset)/10}$

$A(\emptyset)$  = atmosphere attenuation (dB), at any elevation angle, as described above

e. Cosmic Background Adjustment. The noise temperature contribution of the cosmic background is reduced by atmosphere attenuation. For the bands of interest, the effective cosmic background without atmosphere is:

$$\begin{aligned} T_{c,eff} &= 2.7 \text{ K (S-band)} \\ &= 2.5 \text{ K (X-band)} \\ &= 2.0 \text{ K (Ka-band)} \end{aligned}$$

With atmosphere, the net cosmic background effect is:

$$T_c = T_{c,eff}/L \text{ (Kelvins)}$$

where  $L$  = atmosphere loss factor at elevation angle  $\emptyset$ , as given in "d." above

f. Signal-to-Noise Ratio Degradation. The signal-to-noise ratio (SNR) degradation (for atmosphere, ground, and cosmic noise changes) compares system noise temperature and total atmosphere attenuation in the condition (cumulative distribution and elevation angle) of interest to those of some baseline condition, typically, zenith average-atmosphere (CD = 0.25). The SNR degradation is given by:

$$\Delta SNR(\text{dB}) = \Delta A + 10 \log[(T_{base} + \Delta T_{atm} + \Delta T_{ground} + \Delta T_{cosmic})/T_{base}]$$

Note:  $T_{base}$  includes zenith atmosphere, ground, and cosmic noise temperature for CD = 0.25.

g. Example of Use of Attenuation Statistics. The following example shows a typical calculation of atmosphere noise temperature and attenuation for a particular situation.

Example: DSS 43, Canberra  
Ka-band (32 GHz)  
90-percent weather (CD = 0.90)  
20-degrees elevation angle  
T-op at zenith = 20 K (average clear weather)

From Table 3, the zenith attenuation is given as:

$$A_z = 0.4584 \text{ dB}$$

The attenuation at 20-degrees elevation is:

$$A(20) = 0.4584/\sin(20) = 1.3403 \text{ dB}$$

The loss factor L at 20-degrees elevation is:

$$L(20) = 10^{(0.13403)} = 1.3615$$

The atmosphere mean physical temperature is:

$$T_p = 265 + 15 * 0.90 = 278.5 \text{ K}$$

The atmosphere noise temperature at 20-degrees elevation is:

$$T_{atm}(20) = 278.5 * (1 - 1/1.3615) = 73.946 \text{ K}$$

The net cosmic background contribution is:

$$T_c = 2.0/1.3615 = 1.469 \text{ K}$$

The average clear-sky (CD = 0.25) zenith cosmic contribution for an attenuation of 0.1965 dB is 1.912 K. Therefore, the cosmic noise temperature change is -0.443 K. For this example, it is assumed that the ground noise temperature change is +3.0 K.

For a 20 K baseline system noise temperature, the SNR degradation compared to zenith average clear sky condition is given by:

$$\begin{aligned} \Delta \text{SNR} &= (1.3403 - 0.1965) \\ &\quad + 10 \log[(20.0 + 73.946 - 11.888 + 3.0 - 0.443)/20.0] \\ &= 7.408 \text{ dB} \end{aligned}$$

Note that only 1.144 dB is due to attenuation change; the remainder is due to noise temperature effects for this low noise temperature system.

## 2. Wind Loading

The effect of wind loading must be modeled probabilistically, since wind velocity varies randomly over time and space. Figure 3 shows the probability distribution of wind speed for the Goldstone Deep Space Communications Complex. Similar data for the Madrid and Canberra complexes will be supplied when available. The effect of wind load on a particular antenna is dependent on the design of that antenna. Consequently, information on wind load effect on antenna gain is listed in the appropriate antenna module; i.e., TCI-10 for 70-meter antenna stations, TCI-20 for 26-meter antenna stations, and TCI-30 for 34-meter antenna stations.

It is believed that Goldstone is the windiest of the three Deep Space Network antenna complexes. The DSS 14 70-m antenna is stored vertically when wind gusts exceed 45 mile/hr. The frequency of occurrence of this event can be deduced from a relationship between wind gusts and average wind speed. This relationship is found to be: maximum hourly wind speed = 0.62 x strongest gust.

Thus, for 45-mile/hr gusts, the maximum hourly wind speed is found to be 27.9 mile/hr. From Figure 3, it is seen that this speed is exceeded approximately 4 percent (350 hours) of the year and 10 percent (73 hours) of the worst month. Actual practice has shown that no antenna has been stored more than about 10 hours per year due to excessive wind-gust occurrences. During critical tracking periods, wind-gust limitations are expected to be greatly relaxed.

## 3. Hot Body Noise

The increase in system noise temperature when tracking near a radiating body outside the atmosphere can, in principle, be calculated by integrating the blackbody brightness temperature of the source over the antenna gain pattern, which is normalized so that its integral over  $4\pi$  steradians is 1. The resulting temperature must be decreased by the atmospheric attenuation along the antenna beam.

a. Solar Noise. The increase in system noise when tracking near the sun depends on the intensity of solar radiation at the received frequency and on the position of the sun relative to the antenna gain pattern. The quadripod introduces nonuniformities in the sidelobe structure as typically shown in Figure 4. With an azimuth-elevation (AZ-EL) or X-Y mounted antenna, the plane containing the Sun-Earth-Probe (SEP) angle will rotate through the sidelobes during a tracking pass. This causes the solar noise to fluctuate during a track, even if the SEP angle has not changed. With an hour angle-declination (HA-DEC) mounted antenna, the angle between the vertical plane of symmetry of the quadripod and the plane containing the SEP angle remains nearly constant during a tracking pass.

A series of measurements was made at Goldstone in 1987, 1989, and 1990 to determine the system noise temperature effects of tracking near the sun (within about five degrees from the center of the solar disk). These

measurements were made at both S- and X- bands (2295 and 8420 MHz, respectively) on both 26- and 34-meter antennas.

Figure 5 shows the 10.7 cm (2800 MHz) solar radio flux during the last five 11-year solar cycles (NOAA Space Environment Services Center, Solar Geophysical Data). A general characteristic of these curves is a rapid rise to a peak approximately four years after the minimum, followed by a seven-year gradual decrease. It is seen that from cycle-to-cycle, the peak flux can vary by as much as a factor of two. The flux values throughout the cycle at this frequency vary from about 75 SFU (1 solar flux unit =  $1 \times 10^{-22}$  watts/m<sup>2</sup>/Hz) to about 225 SFU. Thus, the 2800 MHz flux is approximately 150 SFU,  $\pm$  75 SFU.

The quiet-sun flux values shown in Figure 5 at 2800 MHz may be modeled to other frequencies between 1 and 10 GHz approximately as  $f^{0.5}$  up to about  $f^1$ . For the active sun, the frequency exponent will likely be lower, down to as low as (-1).

Figure 6 shows X-band system noise temperature increases as measured at the Goldstone DSS-15 HEF antenna. These measurements show the increased effect for the sun located (offset) at right angles to the quadripod legs. These legs are arranged in an "X" configuration, with 90-degree spacing. The measurements were made in November 1987 (near the beginning of the solar cycle) with a measured 2800-MHz flux value of 101 SFU and an 8800-MHz flux value of 259 SFU. This implies a frequency modeling ratio of  $f^{0.8}$ .

Figure 7 shows S-band (2295 MHz) total system noise temperature measurements made on the Goldstone DSS-16 26-meter antenna on December 20, 1989. This antenna has no quadripod; thus, it can be assumed that the noise temperature values shown would be independent of solar "clock angle" around the center of the antenna beam. The reported 2800-MHz solar flux at the time of the experiment was 194 SFU; at 8800 MHz, it was 290 SFU. This flux ratio corresponds to  $f^{0.35}$ .

Figure 8 shows a contour plot of the DSS-12 34-meter HA-DEC antenna S-band total system noise temperature versus declination and cross-declination antenna pointing offsets. The contour interval is 50 K. The quadripod legs are arranged in a "+" configuration with 90-degree spacing. The peaks are at right angles to the legs. These measurements were made on January 12, 1990, when the reported 2800-MHz solar flux was 173 SFU; at 8800 MHz, it was 272 SFU. This flux ratio corresponds to  $f^{0.4}$ .

Figure 9 shows a contour plot of the DSS-12 34-meter HA-DEC antenna X-band total system noise temperature versus declination and cross-declination antenna pointing offsets. The measurement date and flux values are identical with those in Figure 8. The contour interval is 50 K.

From the preceding figures, the following approximate expressions are derived for solar noise temperature increase versus SEP angle:

DSS-16, 26-meter, S-band	$T_{\text{sun}} = 1400 e^{-\theta/0.7}$ (Kelvins)
DSS-12, 34-meter, S-band	$T_{\text{sun}} = 1400 e^{-\theta/0.6}$ (Kelvins)
DSS-12, 34-meter, X-band	$T_{\text{sun}} = 1400 e^{-\theta/0.37}$ (Kelvins)
DSS-15, 34-meter, X-band	$T_{\text{sun}} = 800 e^{-\theta/0.5}$ (Kelvins)

The DSS-15 expression represents an upper limit, for SEP > 0.5 degrees.

These expressions should be compared with the data shown in the corresponding figures to assess their validity. Note that these expressions should be considered valid only for the flux values given above. For predictive purposes, Figure 5 may be used to obtain future 2200-MHz solar flux; this value can then be modeled by frequency.

Figure 10 shows examples of measured S-band system noise temperature made with a 64-meter antenna tracking Pioneer 8 (November 1968, near the solar maximum) and Helios (April 1975, near the solar minimum). For all practical purposes, these curves may be used to predict S-band performance for the DSN 70-meter antennas. The "maximum" and "minimum" curves for each month show the solar "clock angle" effect due to sidelobes at right angles to the quadripod legs.

Figure 11 shows a theoretical curve of X-band 70-meter antenna noise temperature as a function of SEP angle. This curve is generated based on an assumed X-band blackbody disk temperature of 23,000 K, representing an "average" value during the solar cycle. An expression giving quiet sun brightness temperature (K) as a function of wavelength (λ millimeters) has been found to be

$$T_b = 5672 \lambda^{0.24517}$$

For S-band (2.3 GHz),  $T_b = 18700$  K. For X-band (8.5 GHz)  $T_b = 13600$  K. For Ka-band (32 GHz)  $T_b = 9750$  K. The active sun may be expected to have an X-band brightness temperature of as much as 54,000 K, four times as high as the 13600 K calculated above.

b. Lunar Noise. For an antenna pointed near the moon, a noise temperature determination similar to that made for the sun should be carried out. The blackbody disk temperature of the moon is about 240 K, and its apparent diameter is almost exactly that of the sun's (approximately 0.5°). Figures 6 through 11 may be used for lunar calculations, with the noise temperature values scaled by 240/23,000. Figures 7 through 10 include clear sky system noise temperatures which must be subtracted out before scaling in order to determine the noise temperature increase.

c. Planetary Noise. The increase in system noise temperature ( $T_{p1}$ ) when tracking near a planet can be calculated by the formula

$$T_{p1} = \frac{T_K G D^2}{16 R^2} e^{-2.77 \left( \frac{\theta}{\theta_0} \right)}$$

where  $T_K$  = blackbody disk temperature of the planet, K

$G$  = antenna gain, ratio, including atmospheric attenuation

$D$  = planet diameter, km

$R$  = distance to planet, km

$\theta$  = angular distance from planet center to antenna beam center

$\theta_0$  = antenna half-power beamwidth (full beamwidth at half power)

Table 4 presents all the parameters needed for calculation of planetary noise contributions. Also given are maximum and minimum values of expected noise contributions for inferior and superior conjunctions, respectively, with the antenna beam pointed at the center of the planet ( $\theta = 0$ ). Corresponding

S-band noise temperature increases will be approximately 1/14 as large as the X-band increases because of the lower antenna gain (wider beamwidth) at the lower frequency.

In the case of Jupiter, there is a significant and variable non-thermal component of the noise temperature. Thus, the effective blackbody disk temperature at S-band appears to be much higher than that at X-band. The S-band noise temperature increase will be approximately 1/6 the X-band values for average Jupiter emission; or about 1/3 the X-band values for maximum Jupiter emission.

For Venus at Ka-band, the blackbody disk temperature is 475 K.

The expression  $T_{p1}$  assumes that the angular extent of the radiating source is small compared to the antenna beamwidth. This approximation is adequate except for Venus near-inferior conjunction and a 70-meter antenna at X-band (Venus apparent diameter =  $0.018^\circ$ , beamwidth =  $0.035^\circ$ ). It is also assumed that the antenna main beam has a Gaussian shape, with circular symmetry. Antenna gains and half-power beamwidths are given in TCI-10, -20, and -30.

Table 4. Parameters for X-band Planetary Noise Calculation plus  
Sample X-band Noise Temperature Contributions

Planet	Diameter (km) Polar x Equatorial)	Distance from Earth (10 <sup>6</sup> km)		Mean Distance from Sun (10 <sup>6</sup> km)	Blackbody Disk Temperature (K)	X-band Planetary Noise Temperature (K)			
		Superior Conj	Inferior Conj			70-m Antenna, G = 74.2 dBi		34-m Antenna, G = 68.3 dBi	
						Superior Conj	Inferior Conj	Superior Conj	Inferior Conj
Mercury	4840	220	78.8	57.9 (0.387 AU)	625	0.50	3.86	0.12	1.00
Venus	12400	261	38.6	108.1 (0.723 AU)	648	2.40	110.00	0.62	28.23
Earth	12757	-	-	149.6 (1.000 AU)	250-300	-	-	-	-
Mars	6800	399	56.3	227.8 (1.524 AU)	192	0.10	4.80	0.03	1.23
Jupiter	133874 x 142740	967	589	778 (5.202 AU)	234*	7.86	21.17	2.01	5.45
Saturn	109184 x 120800	1657	1197	1426 (9.539 AU)	155-180**	1.43	2.72	0.37	0.11
Uranus	44119 x 47060	3157	2586	2868 (19.18 AU)	215	0.08	0.11	0.03	0.03
Neptune	43708 x 44600	4685	4309	4494 (30.06 AU)	200	0.03	0.03	<0.02	<0.02
Pluto	6400***	7546	4272	5896 (39.44 AU)	≈200	<0.02	<0.02	<0.02	<0.02

\* 87% thermal, 13% non-thermal from radiation belts

\*\* Depending on inclination of rings

\*\*\* Uncertain

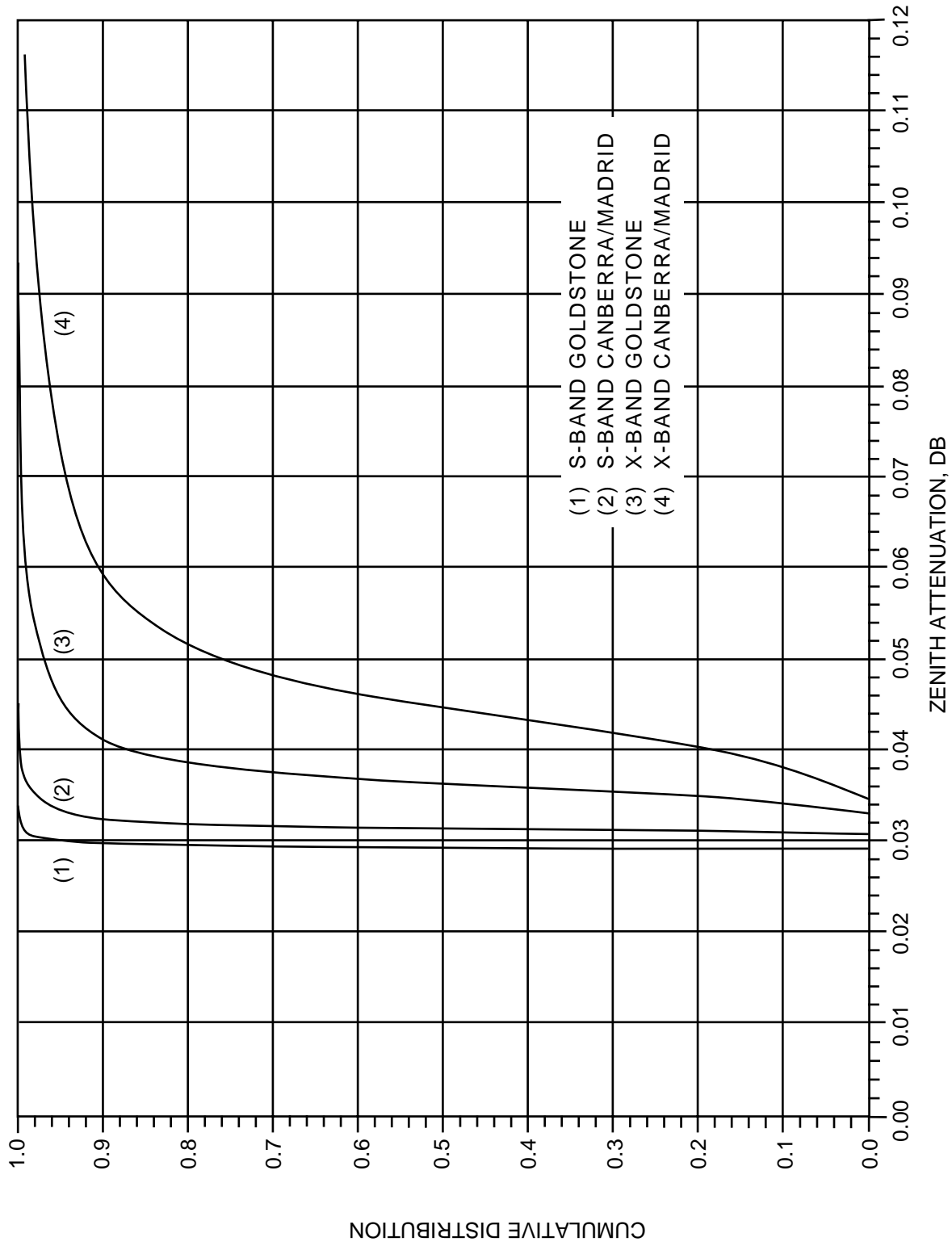


Figure 1. Cumulative Distribution of Total Zenith Attenuation for S-band and X-band

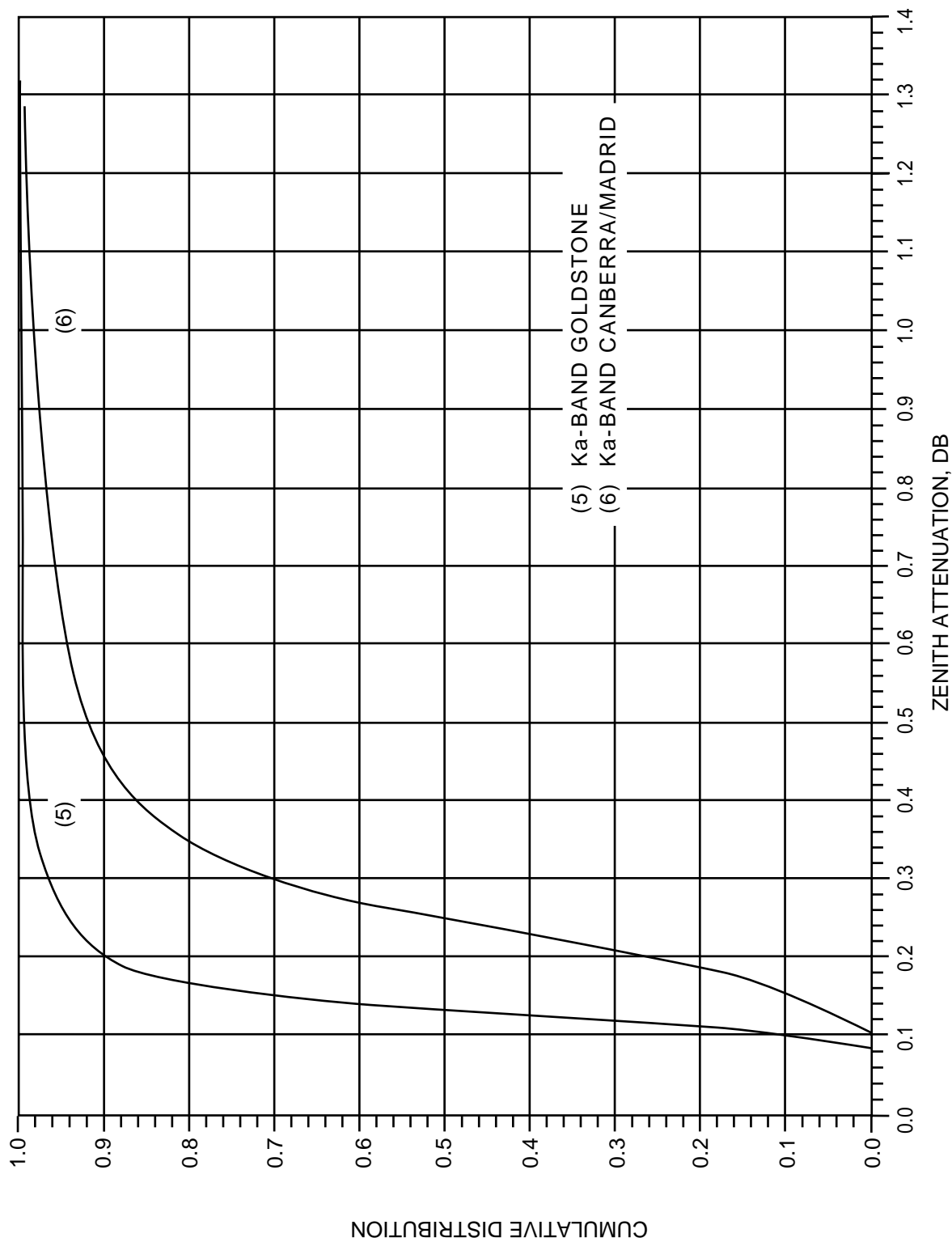


Figure 2. Cumulative Distribution of Total Zenith Attenuation for Ka-band

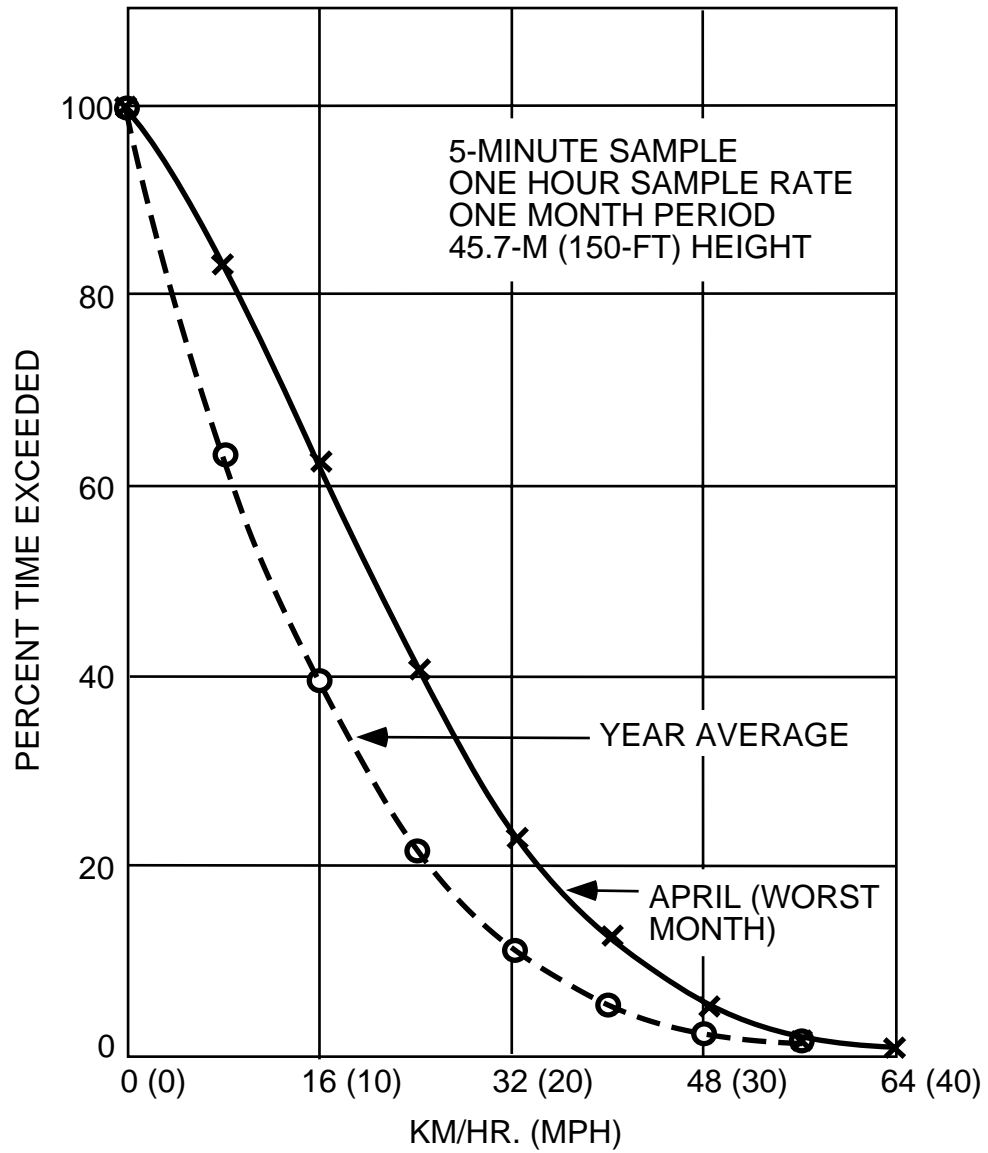


Figure 3. Probability Distribution for Wind Conditions at Goldstone

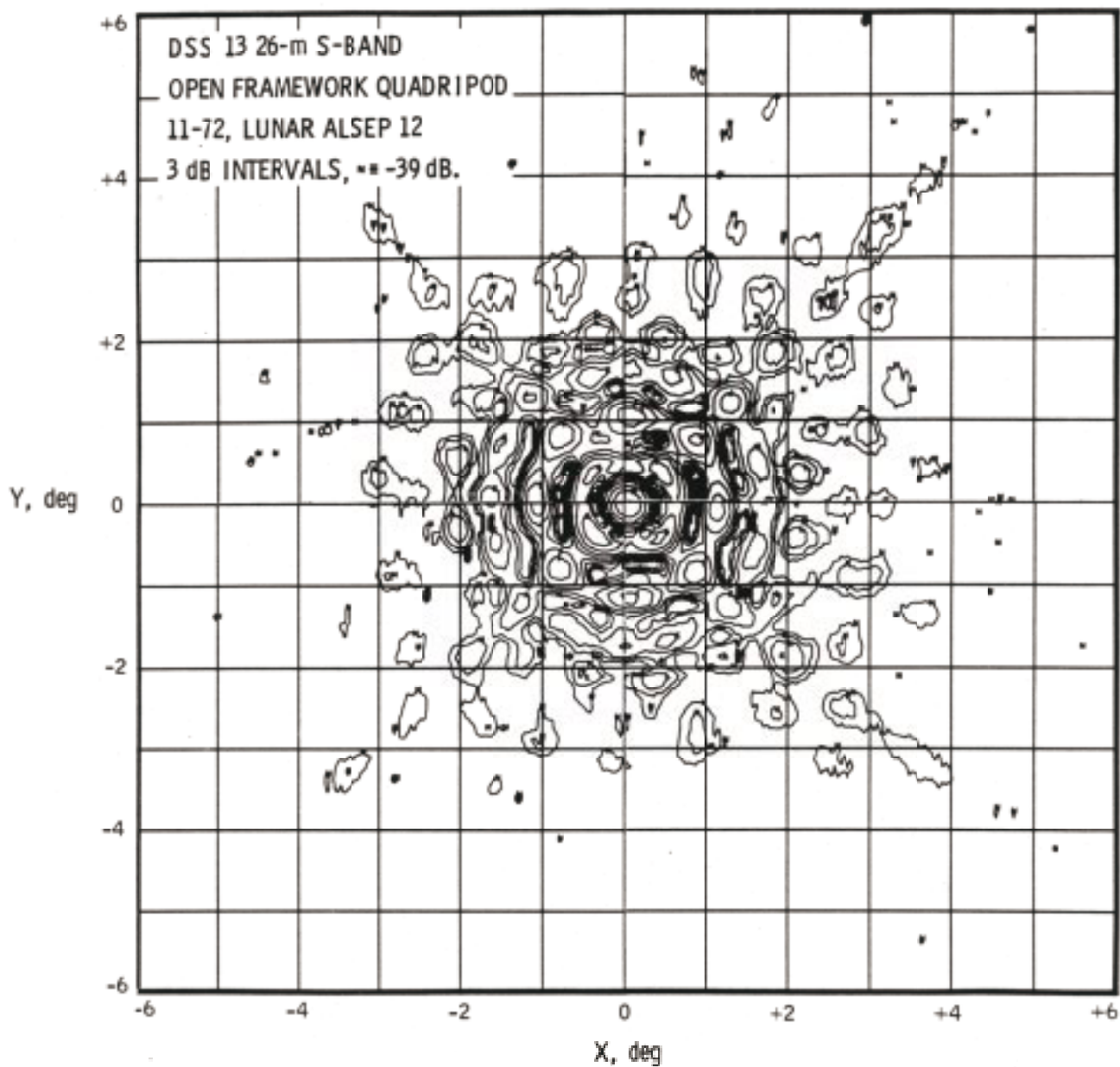


Figure 4. Typical 26-meter S-band Antenna Pattern Showing Sidelobe Structure

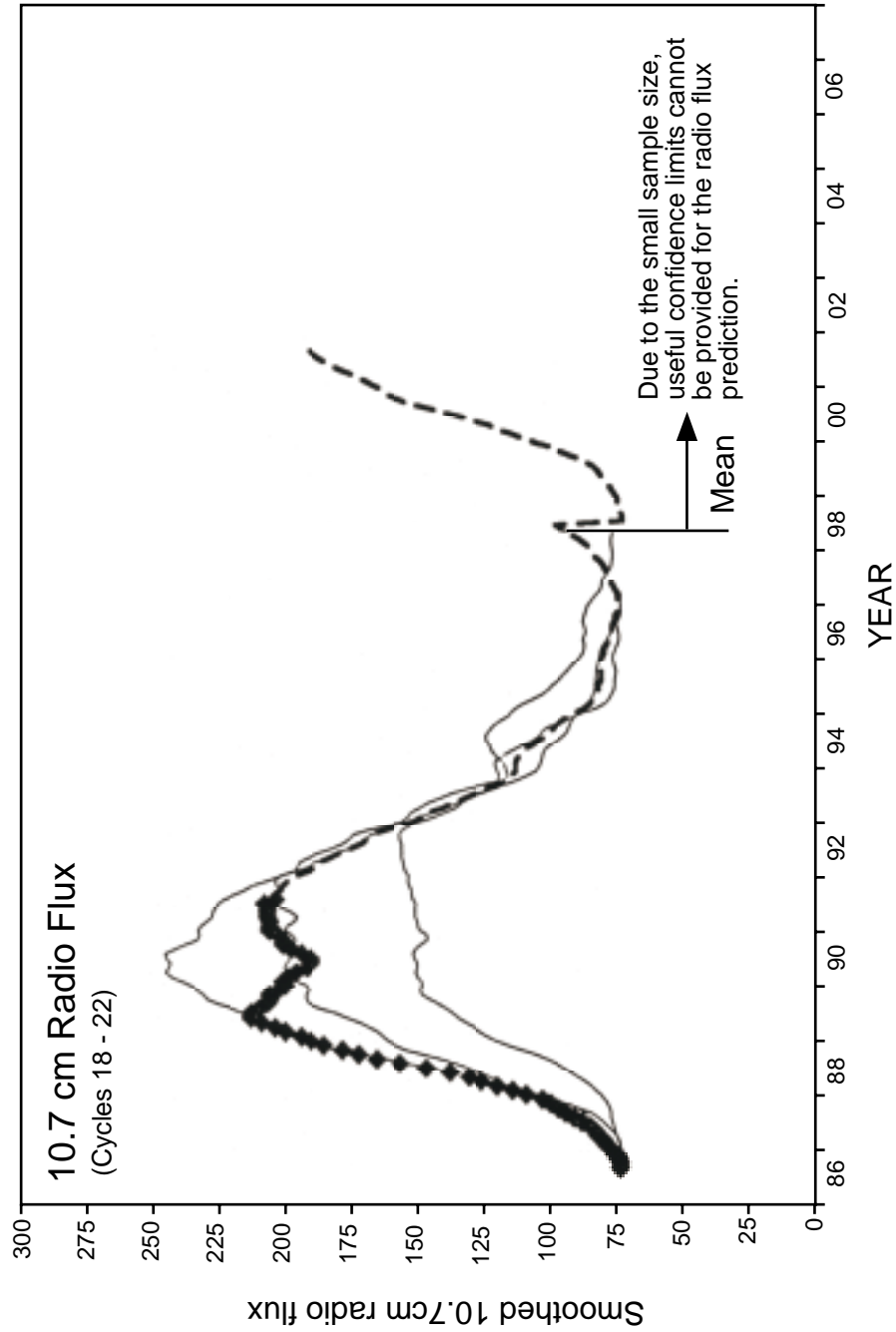


Figure 5. Solar Radio Flux (SFU) at 2800 MHz (10.7 cm Wavelength)  
During Solar Cycles 18 Through 22 (Present)

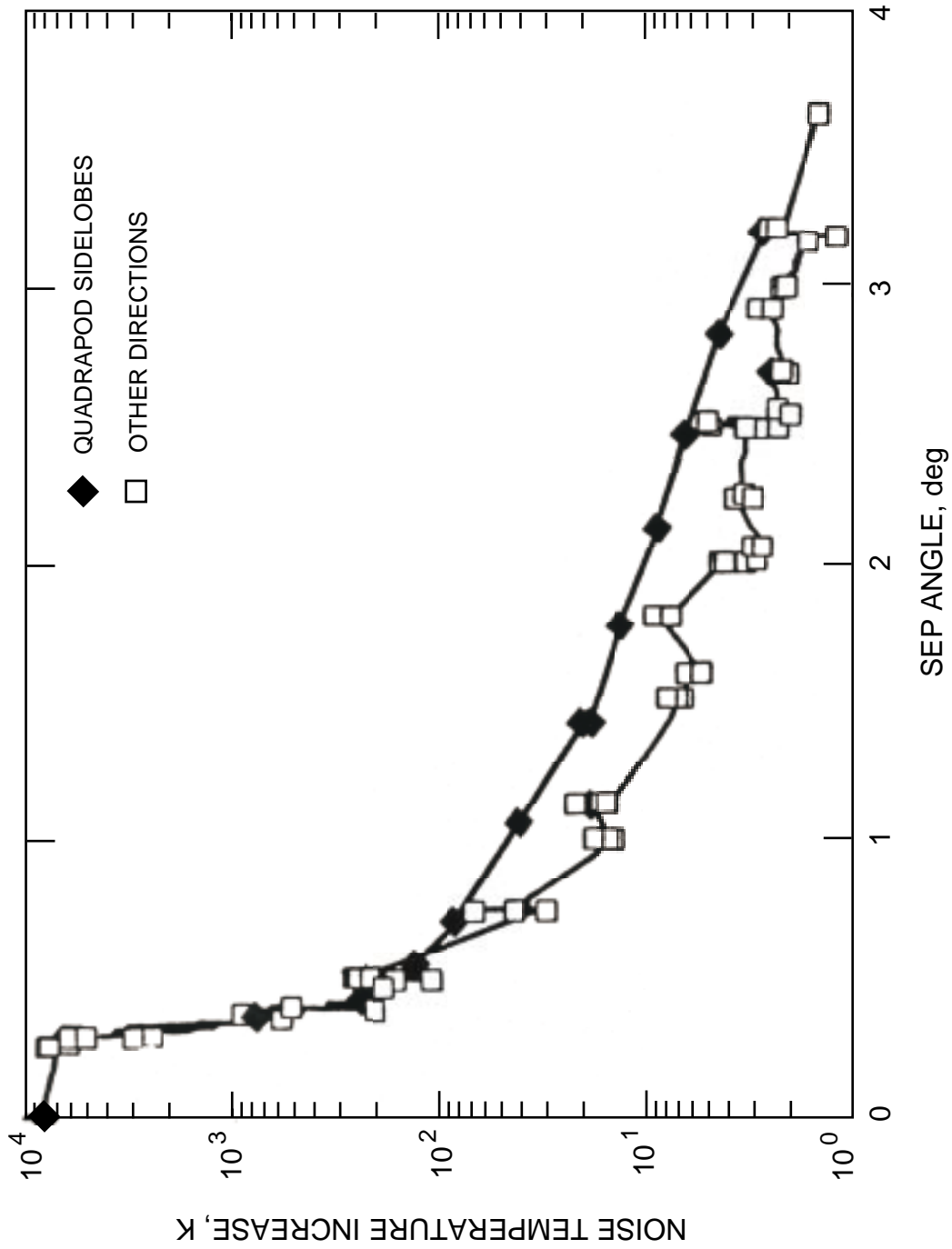


Figure 6. DSS-15 X-band System Noise Temperature Increased Due to the Sun at Various Offset Angles, Showing Larger Increases Perpendicular to Quadrapod Directions

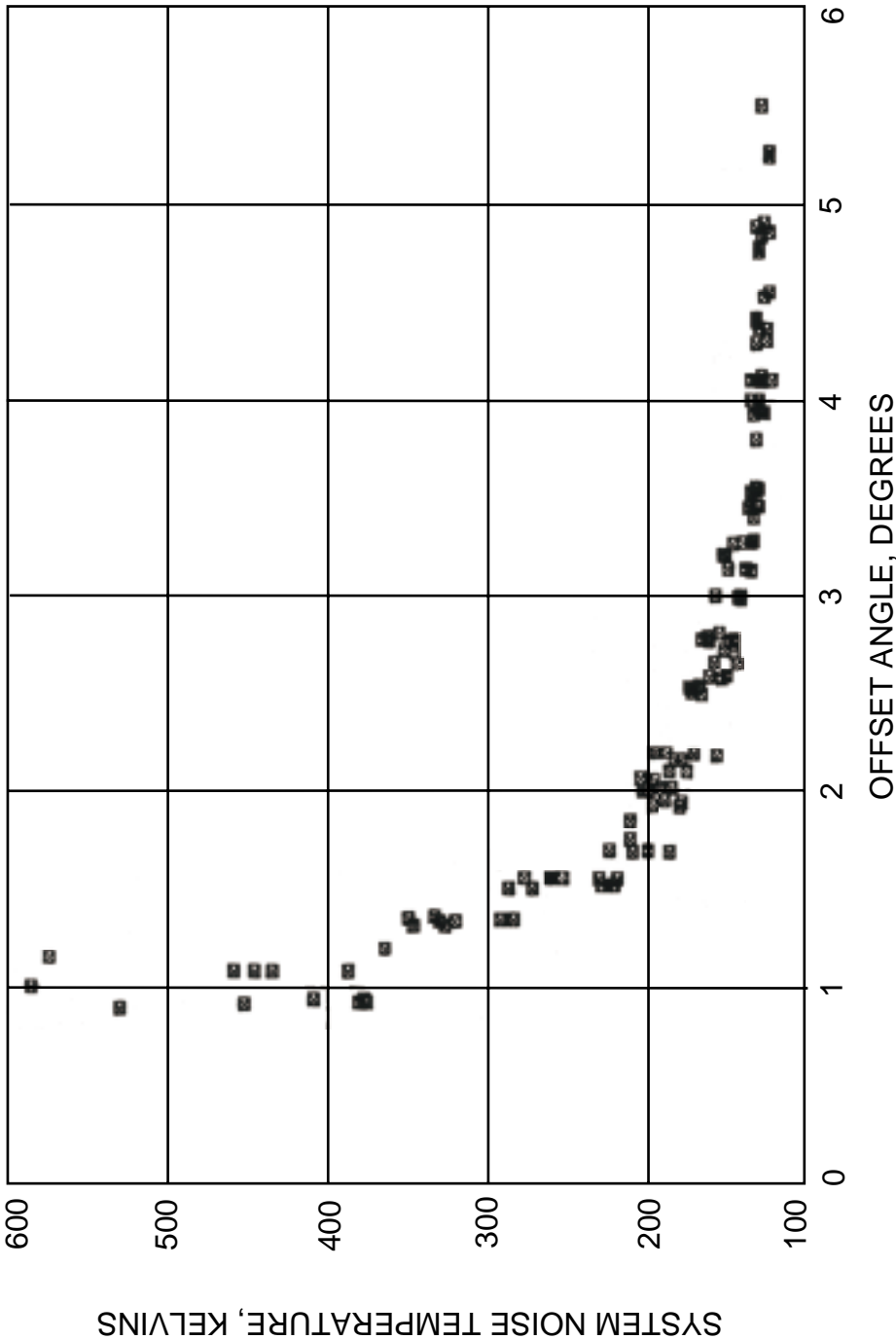


Figure 7. DSS-16 S-band Total System Noise Temperature at Various Offset Angles from the Sun

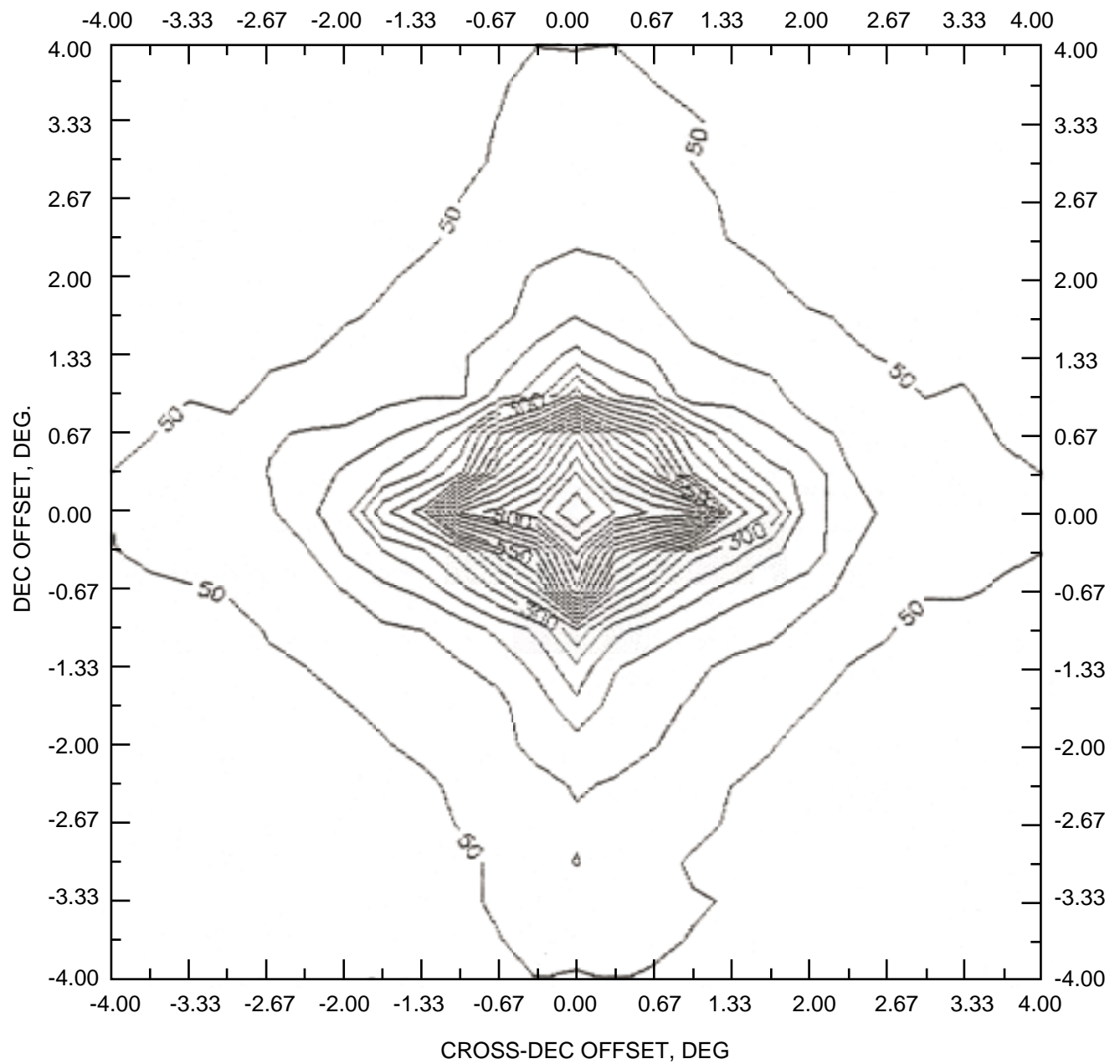


Figure 8. DSS-12 S-band Total System Noise Temperature at Various Declinations and Cross-Declination Offsets from the Sun

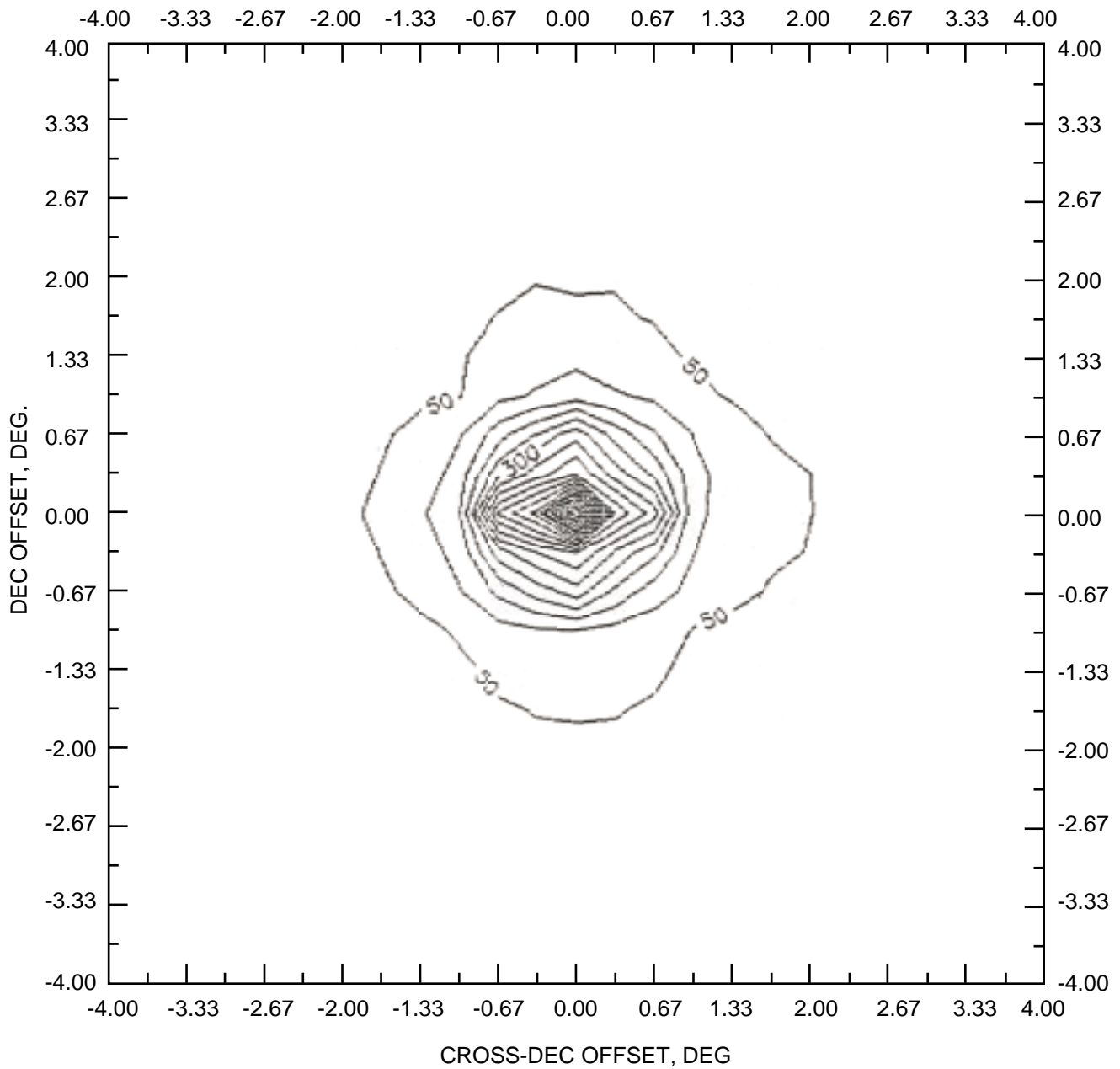


Figure 9. DSS-12 X-band Total System Noise Temperature at Various Declination and Cross-Declination Offsets from the Sun

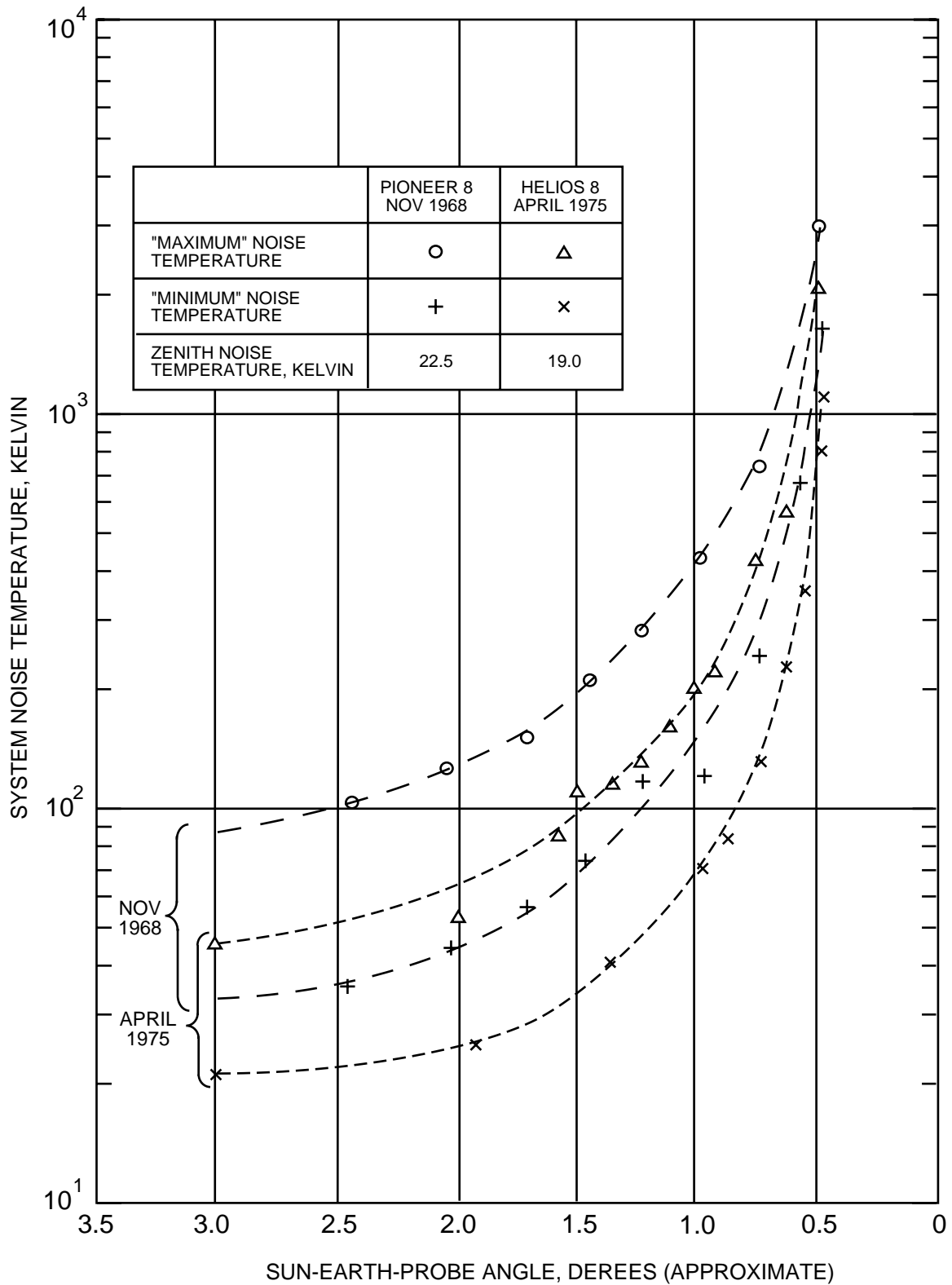


Figure 10. Total S-band Total System Noise Temperature for 70-meter Antennas Tracking Spacecraft Near the Sun (Derived from 64-meter measurements)

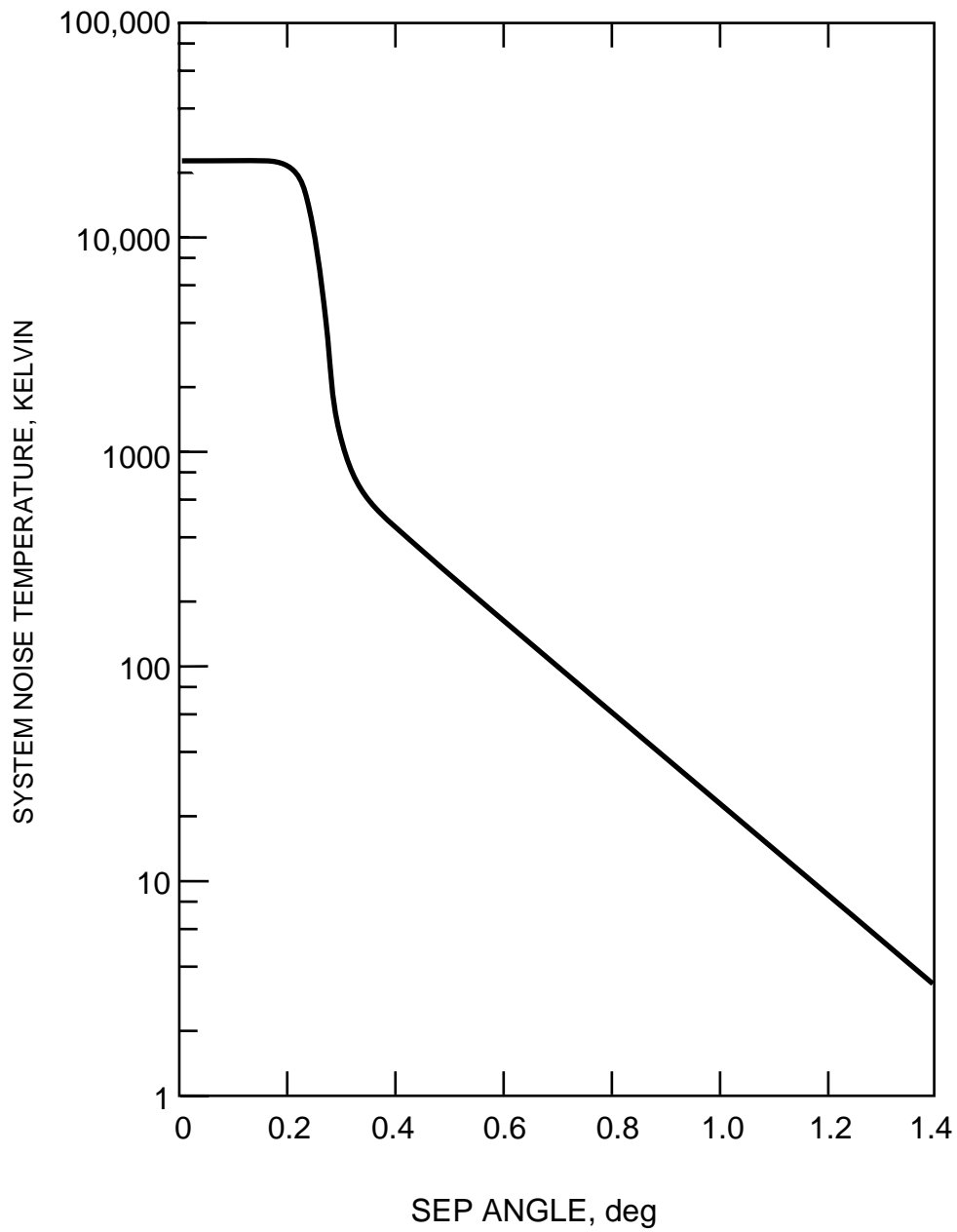


Figure 11. X-band Noise Temperature Increase for 70-meter Antennas as a Function of SEP Angle, Nominal Sun, 23,000 K Disk Temperature